Supporting information

A Buoyant Plasmonic Microbubble-based SERS Sensing platform for Amyloid-beta Protein Detection in Alzheimer's Disease

Willis Kwun Hei Ho[a†], Qin Zhang[a,b†*], Fariza Zhorabe[e], Jiaxiang Yan[a], Yutian Gu[a], Shujun Wang[a], Changqing Yi[f], Yu Zhang[g], Mo Yang[a,b,c,d *]

[a] Department of Biomedical Engineering, The Hong Kong Polytechnic University, Hong Kong 999077, China

[b] The Hong Kong Polytechnic University Shenzhen Research Institute, Shenzhen 518000, China

[c] Research Center for Nanoscience and Nanotechnology, The Hong Kong Polytechnic University, Kowloon, Hong Kong 999077, China

[d] Joint Research Center of Biosensing and Precision Theranostics, The Hong Kong Polytechnic University, Kowloon, Hong Kong 999077, China

[e] Department of Chemical and Biological Engineering, The Hong Kong University of Science and Technology, Hong Kong 999077, China

[f] Key Laboratory of Sensing Technology and Biomedical Instruments (Guangdong Province), School of Biomedical Engineering, Sun Yat-Sen University, Guangzhou 510000, China

[g] Department of Mechanical and Automotive Engineering, Royal Melbourne Institute of Technology, Melbourne VIC 3000, Australia

***Corresponding Authors**:
Qin Zhang: qin7zhang@polyu.edu.hk
Mo Yang: mo.yang@polyu.edu.hk

† Willis Kwun Hei Ho and Qin Zhang contributed equally to this work.

Keywords: Surface-enhanced Raman spectroscopy, PVA microbubbles, plasmonic coupling, amyloid-β, Alzheimer disease

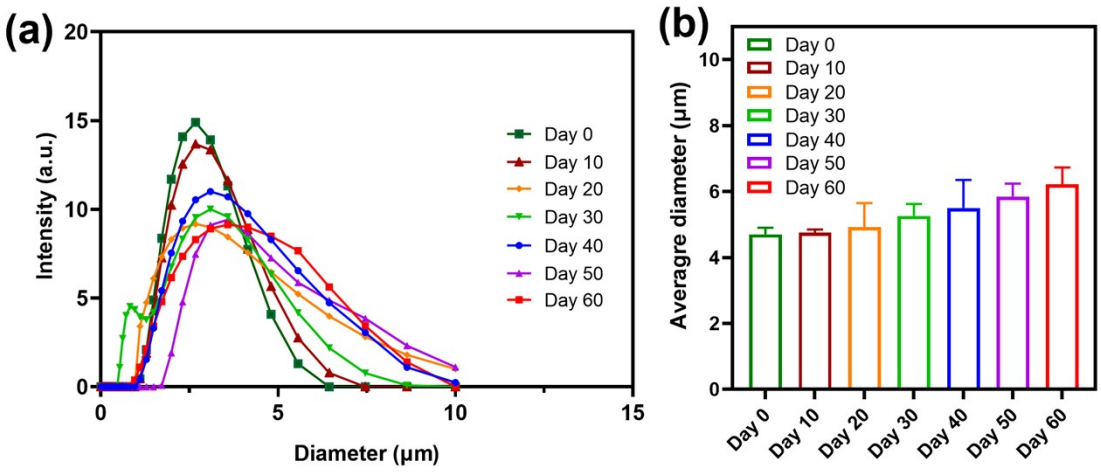

Fig. S1 (a) Size distribution of PVA microbubbles measured by dynamic light scattering (DLS). PVA microbubbles were dispersed in PBS and stored at 4℃. (b) The average diameter of PVA microbubbles in PBS measured by DLS at different time.

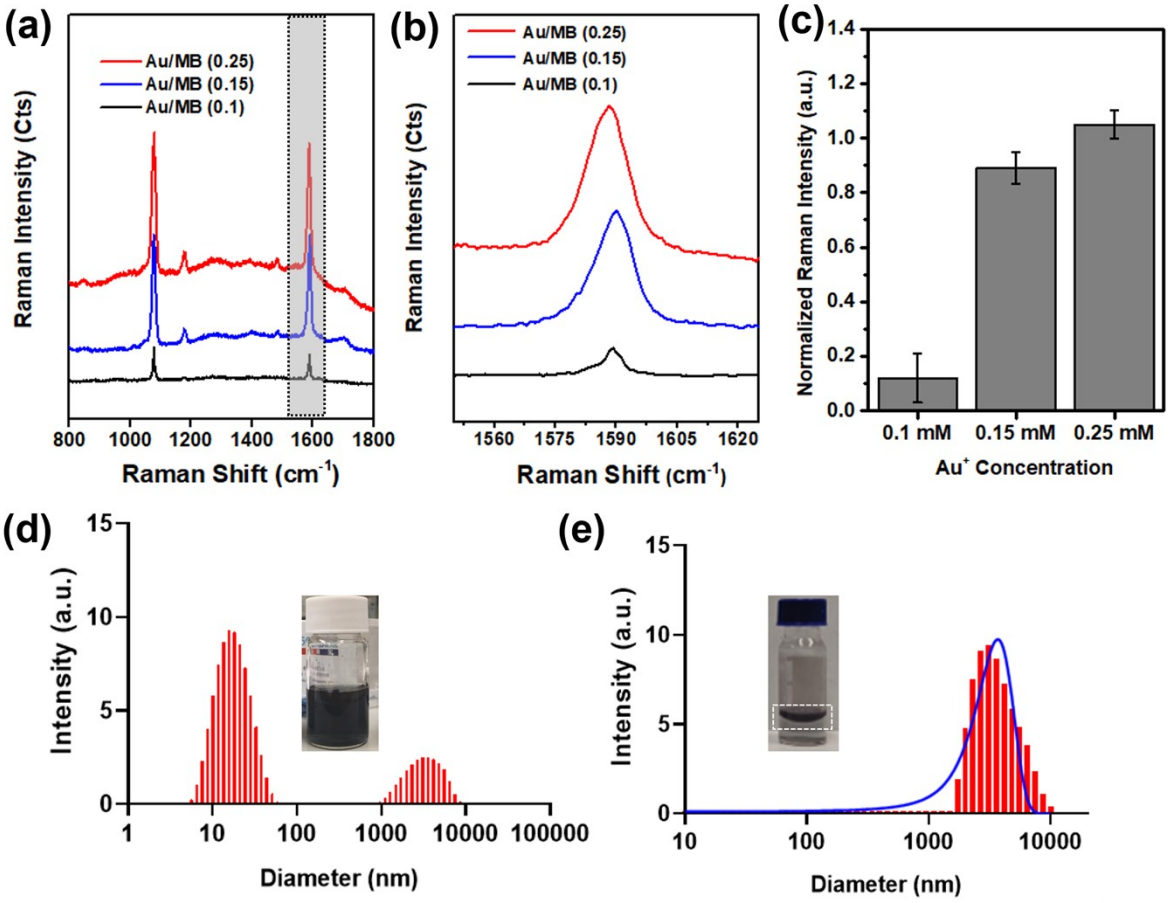

Fig. S2 (a) SERS Raman spectra of 4-MBA on Au/MB substrates prepared with different Au^{+} concentrations (0.1, 0.15, 0.25 mM). (b) Zoomed-in SERS spectra of (a). (c) The normalized Raman signal intensity at ~1590 cm^{-1} measured at Au/MB substrates prepared with different

Au^{+} concentrations. (d) DLS distribution of Au/MB prepared with 0.4 mM Au^{+} precursor dispersed in H_2O for 2 days. Inset: photograph of Au/MB (0.4 mM). (e) DLS distribution of Au/MB prepared with 0.25 mM Au^{+} precursor dispersed in H_2O. Inset: photograph of Au/MB (0.25 mM).

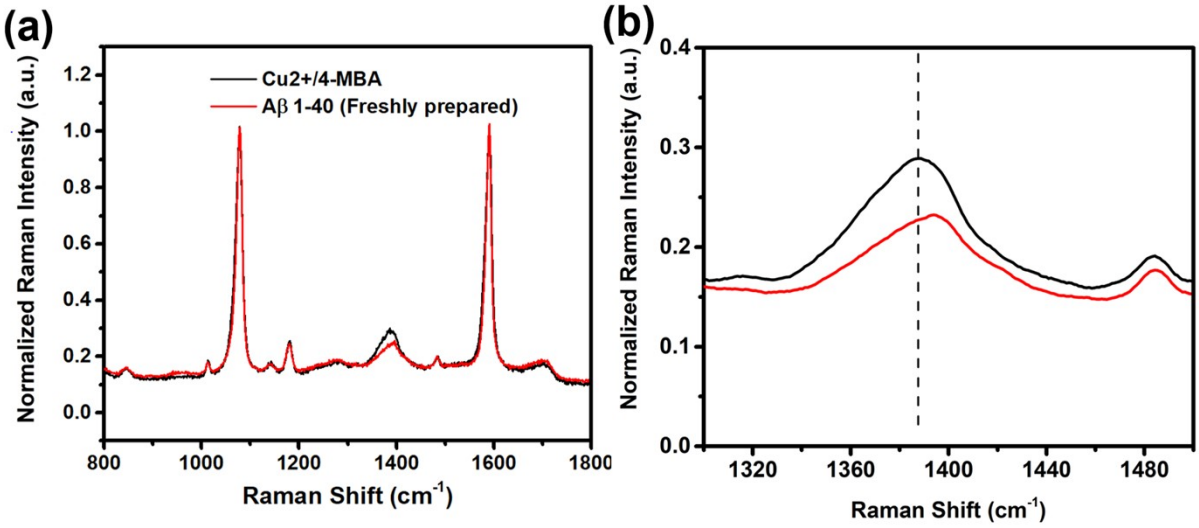

Fig. S3 (a) Raman spectra of the Cu^{2+}/4-MBA/Au/MB sensing platform before and after incubation with freshly prepared $A\beta_{1\text{-}40}$ monomers at a concentration of 10^{-6}M. (b) The enlarged 4-MBA spectra (1300cm^{-1}-1500 cm^{-1}).

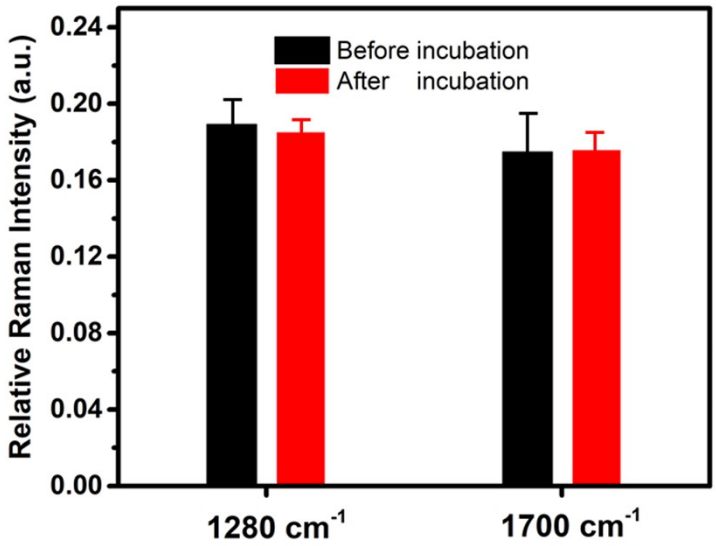

Fig. S4 Protonated associated carboxyl group peak intensity before (Black) and after (Red) the incubation with $A\beta_{1\text{-}40}$ oligomers.

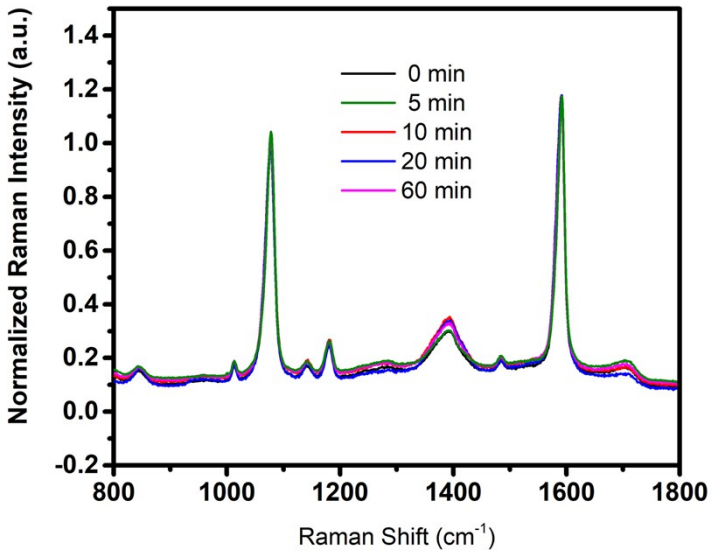

Fig. S5 Raman spectra of the Cu^{2+}/4-MBA/Au/MB sensing platform after incubation in protein dilute buffer (PBS, 10 mM) over time.

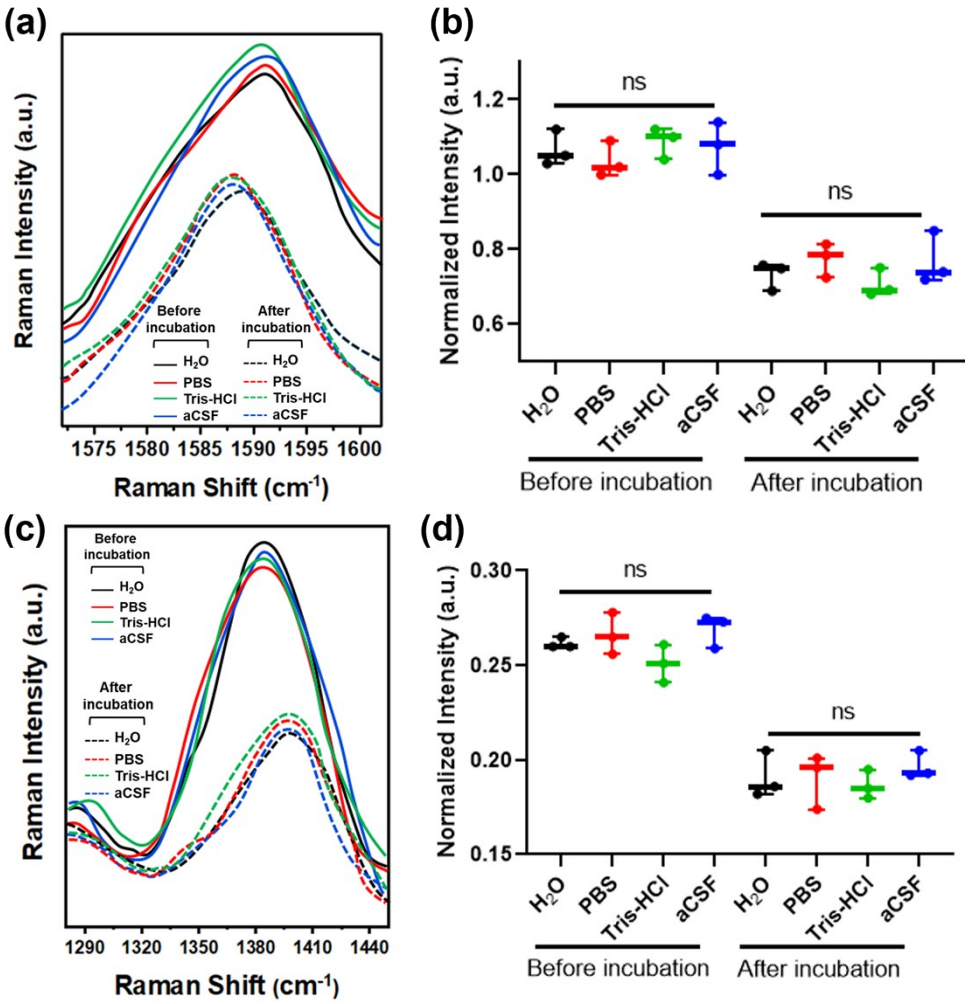

Fig. S6 (a) The υ8a band in the SERS spectra of Cu^{2+}/4-MBA/Au-MB sensing system before and after incubation with $A\beta_{1\text{-}40}$ protein at a concentration of 10^{-6} M in H_2O (black line), PBS (red line), Tris-HCl (green line), and artificial cerebrospinal fluid (aCSF, blue line). (b) The normalized peak intensity of υ8a vibration (~1592 cm^{-1}). (c) The $\upsilon_s(COO^{-}–Cu^{2+})$ band in the SERS spectra of Cu^{2+}/4-MBA/Au-MB sensing system before and after incubation with $A\beta_{1\text{-}40}$ protein at a concentration of 10^{-6} M in H_2O, PBS, Tris-HCl, and aCSF buffer. (d) The normalized peak intensity of $\upsilon_s(COO^{-}–Cu^{2+})$ band (~1388 cm^{-1}).

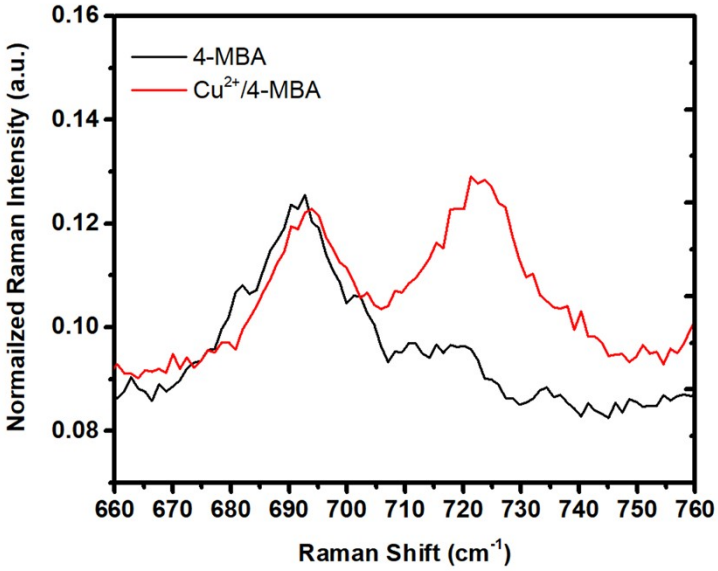

Fig. S7 Raman spectra of 4-MBA in Au/MB substrate before (black line) and after (red line) coordination with Cu^{2+} ions.

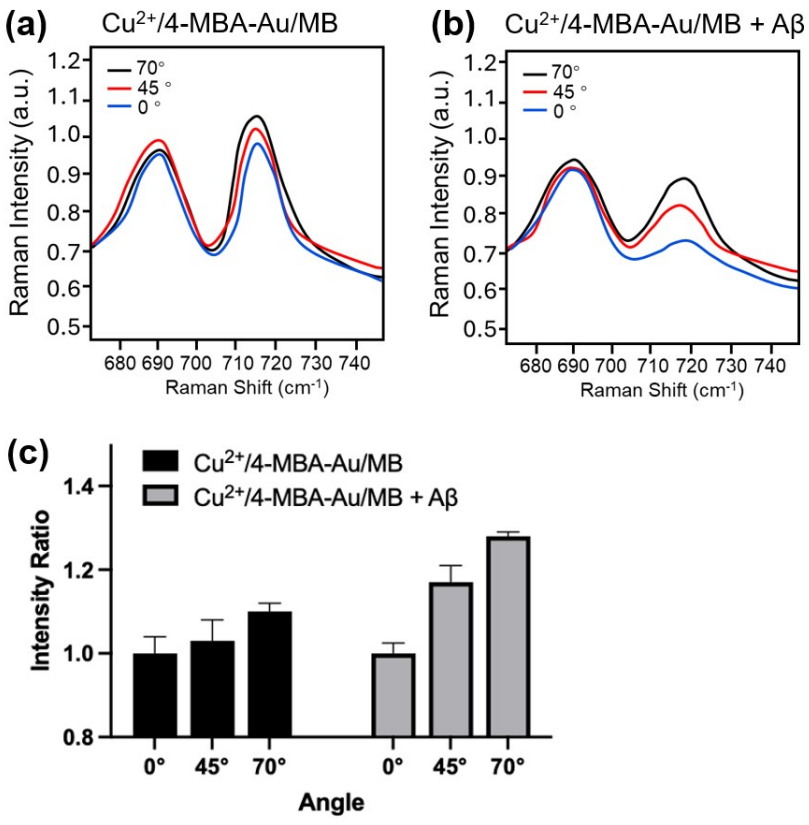

Figure S8. Raman spectra of the out-of-plane υ(CCC) bending mode (~718 cm^{-1}) for (a) Cu^{2+}_4-MBA_Au/MB platform, and (b) Cu^{2+}_4-MBA_Au/MB platform after incubation with $A\beta_{1\text{-}40}$ protein at a concentration of 10^{-6} M. The angle-resolved SERS measurements were

conducted by collecting Raman spectra at angles of 0°, 45°, and 70° relative to the substrate coated in silicon. (c) Ratio of normalized signal intensity of the υ(CCC) band calculated as $I_{45°}/I_{0°}$ and $I_{70°}/I_{0°}$ for both sample groups.

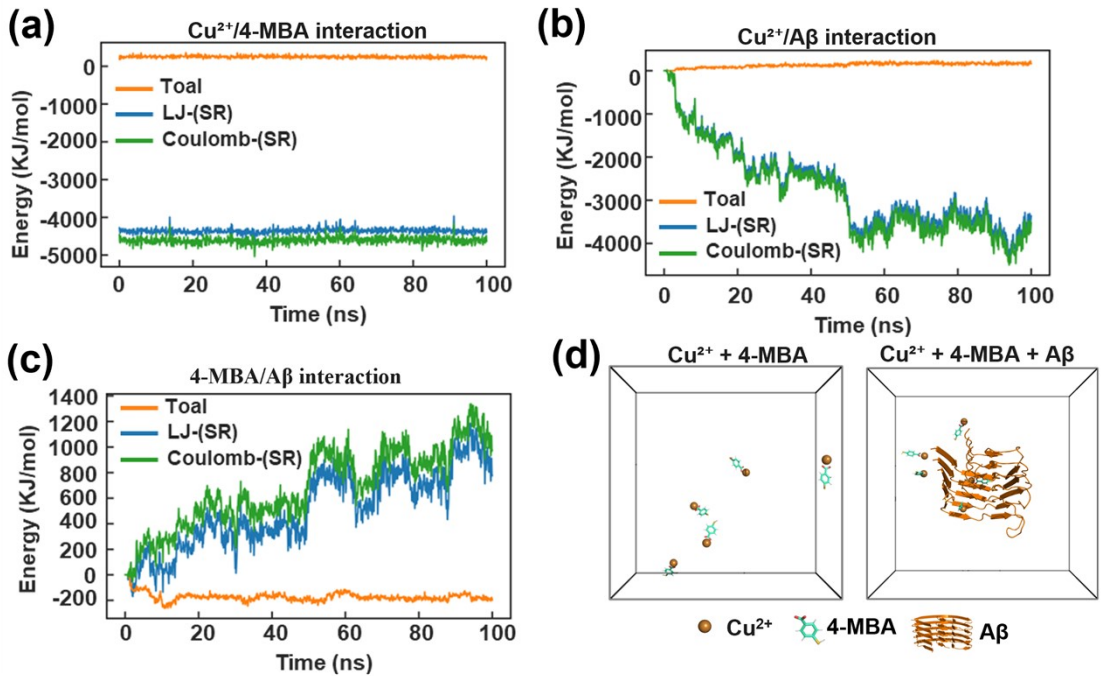

Fig. S9 Time evolution of van der Waals and electrostatic interaction energies between different molecular pairs during the molecular dynamics (MD) simulation. (a) Cu^{2+}/4-MBA interaction; (b) Cu^{2+}/Aβ interaction; (c) 4-MBA/Aβ interaction. LJ-SR energy reflects short-range van der Waals interactions, while Coulomb-SR energy represents the electrostatic interaction between charged atoms. (d) Snapshots of the MD simulation system at 100 ns before and after the introduction of the Aβ peptide, illustrating intermolecular interactions, molecular trajectories, and the overall structural change.

Table S1. Au nanostructure-based SERS platform and ELISA assay-based sensing technologies for disease-associated protein detection.

Sensing platform	Methods	Analytes	LoD	Time required	Matrix	Ref.
Plasmonic Au NRs-based substrate	SERS	BSA	50 nM	10-60 min	PBS	[1]
Ag/Au plasmonic hybrid nanoarray	SERS	Hemoglobin	5 ng/mL	20 min	Urine	[2]
Gold nanostars (AuNS) substrate	SERS	Protein kinase A	5 mU/mL (~83.3 ng/mL)	Not mentioned	PBS	[3]
AuNP-WS2 Nanohybrid	SERS	myoglobin	100 ng/mL	15 min	Tris-HCl	[4]
Au NPs -decorated polystyrene beads	SERS	Amyloid oligomers	100 nM	Not mentioned	PBS	[5]
Two layers of Au NPs (Au@RRs@AuNPs)	SERS	$A\beta_{1-42}$	0.3 nM (1.2 ng/mL)	Not mentioned	aCSF	[6]
Plasmonic ELISA-based immunoassay	ELISA	$A\beta_{1-40}$	50 pM	> 2 h	CSF	[7]
Commerial $A\beta_{1-40}$ ELISA Kit from Abcam company	ELISA	$A\beta_{1-40}$	0.1 ng/mL	6-8 h	CSF	[8]
Au NPs /microbubbles-based substrate	SERS	$A\beta_{1-40}$	1 nM (~4.3 ng/mL)	30 min	Acsf	This work

References

1. A. Foti, C. D'Andrea, V. Villari, N. Micali, M. G. Donato, B. Fazio, O. M. Marago, R. Gillibert, M. Lamy de la Chapelle and P. G. Gucciardi, *Materials (Basel)*, 2018, **11**, 440.
2. J. Wu, Y. Zhang, J. Wang, Z. Ling, X. Yan, X. Lyu, J. Fang, M. Cheng, M. Zhao, T. Ban, Y. Liu and Y. Li, *Anal. Chem.*, 2024, **96**, 15735-15745.
3. S. He, Y. M. E. Kyaw, E. K. M. Tan, L. Bekale, M. W. C. Kang, S. S. Kim, I. Tan, K. P. Lam and J. C. Y. Kah, *Anal. Chem.*, 2018, **90**, 6071-6080.
4. M. Shorie, V. Kumar, H. Kaur, K. Singh, V. K. Tomer and P. Sabherwal, *Mikrochim Acta*, 2018, **185**, 158.
5. L. Guerrini, R. Arenal, B. Mannini, F. Chiti, R. Pini, P. Matteini and R. A. Alvarez-Puebla, *ACS Appl. Mater. Interfaces*, 2015, **7**, 9420-9428.

6. C. Dallari, E. Lenci, A. Trabocchi, V. Bessi, S. Bagnoli, B. Nacmias, C. Credi and F. S. Pavone, *ACS Sens.*, 2023, **8**, 3693-3700.
7. M. Li, D. Lu, R. You, H. Shen, L. Zhu, Q. Lin and Y. Lu, *J. Phys. Chem. C*, 2022, **126**, 12651-12659.
8. H. Li, Y. Tian, S. Yan, L. Ren, R. Ma, W. Zhao, H. Zhang and S. Dou, *Coatings*, 2024, **14**, 530.